

SWEET-Cat update and MOOGme

A new minimization procedure for high quality spectra

D. T. Andersen^{1,2}, S. G. Sousa¹, N. C. Santos^{1,2}, M. Tsantaki³, G. Teixeira¹, L. Suárez-Andrés^{4,5}, and A. Mortier⁶

¹ Instituto de Astrofísica e Ciências do Espaço, Universidade do Porto, CAUP, Rua das Estrelas, 4150-762 Porto, Portugal e-mail: daniel.andreasen@astro.up.pt

² Departamento de Física e Astronomia, Faculdade de Ciências, Universidade do Porto, Rua Campo Alegre, 4169-007 Porto, Portugal

³ Instituto de Radioastronomía y Astrofísica, IRyA, UNAM, Campus Morelia, A.P. 3-72, 58089 Michoacán, Mexico

⁴ Instituto de Astrofísica de Canarias, E-38205 La Laguna, Tenerife, Spain

⁵ Depto. Astrofísica, Universidad de La Laguna (ULL), E-38206 La Laguna, Tenerife, Spain

⁶ SUPA, School of Physics and Astronomy, University of St Andrews, St Andrews KY16 9SS, UK

Received ...; accepted ...

ABSTRACT

Aims.

Methods.

Results.

Key words. data reduction: high resolution spectra – stars individual: Arcturus – stars individual: HD010853

1. Introduction

The study of extrasolar planetary systems is an established field of research. To date, over 3200 extrasolar planets have been discovered around solar-type stars¹. Most of these have been found thanks to the incredible precision achieved in photometric transit and radial velocity. Especially the latest announcement from the *Kepler* space mission with 1284 confirmed exoplanets (Morton et al. 2016). The increasing number of exoplanets allow us to do statistical studies of the newfound worlds by analyzing their internal structure, atmospheric composition, with more.

A key aspect to this progress is the characterization of the planet host stars. For instance, precise and accurate stellar radii are critical if we want to measure precise values of the radius of a transiting planet (see e.g. Torres et al. 2012). The determination of the stellar radius is in turn dependent on the quality of the derived stellar parameters such as the effective temperature.

We continue the work of Santos et al. (2013) by deriving parameters in a homogeneous way using the method described in Sousa et al. (2011).

2. MOOGme

MOOGme (acronym for MOOG made easy) is a web tool for analyzing spectra. MOOGme is written in Python and works as a wrapper around MOOG (Snedden 1973), and ARES (Sousa et al. 2015) for an all-in-one tool. MOOG is a radiative transfer code under the assumption of local thermodynamic equilibrium (LTE). And ARES is a tool to measure equivalent widths (EW) automatically from a spectrum given a line list. MOOGme has

four different functions: Measure EWs with ARES, synthetic fitting, EW method, and abundances, all described below. We use the Kurucz atmospheric grid from Kurucz (1993).

2.1. EW measurements

EW measurements are important for the EW method and to obtain abundances. This can be done manually using a tool like IRAF, but often when dealing with a large sample of stars this is not a suitable way to deal with the problem. Therefore tools like ARES exists which can measure the EW of spectral lines automatically. To use this mode of MOOGme, ARES has to be installed and be in the PATH. Then MOOGme just need a spectrum (format should be 1D for ARES to read it) and a line list. For the latter, MOOGme is shipped with some line lists ready to use, in the format suitable for MOOGme. The output will be a line list in the format required for MOOG. The output can be used for either the EW method or the abundance method, both described below.

2.2. EW method

This is a standard method for obtaining parameters from stellar spectra. Here measured EWs are used to calculate abundances using a given stellar atmosphere model with a given set of atmospheric parameters, effective temperature (T_{eff}), surface gravity ($\log g$), metallicity ($[\text{Fe}/\text{H}]$, where iron often is used as a proxy), and the micro turbulence (ξ_{micro}). By removing correlations between the measured abundances (through the measured EWs) and the excitation potential and reduced EW ($\log(EW/\lambda)$) we can constrain T_{eff} and ξ_{micro} . By obtaining ionization balance between Fe I and Fe II, that is the average abundance of all Fe I lines

¹ For an updated table we refer to <http://www.exoplanet.eu>

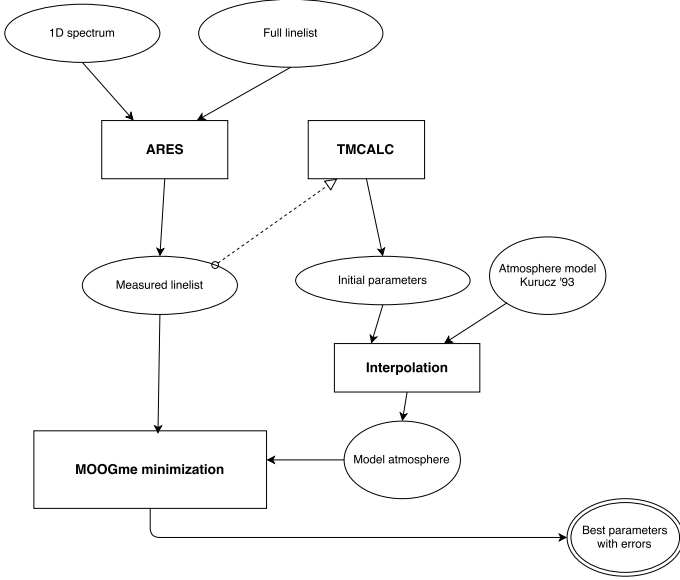


Fig. 1. A general overview over MOOGme from spectrum to parameters.

are equal to the average abundance of all Fe II lines, we constrain $\log g$. Last, we change the input $[\text{Fe}/\text{H}]$ to match that of the average output $[\text{Fe}/\text{H}]$. Hence we have four criteria to minimize simultaneously:

1. The slope between abundance and excitation potential ($a_{\text{EP}} \leq 0.001$).
2. The slope between abundance and reduced EW ($a_{\text{RW}} \leq 0.003$).
3. The difference between the average abundances of Fe I and Fe II ($\Delta\text{Fe} = 0.00$).
4. Input and output metallicity should be equal.

These criteria we denote as indicators for the physical parameters we are trying to minimize for.

There exists many minimization routines available in Python. Most commonly known are the ones from the SciPy ecosystem². There are some pros and cons with using proprietary minimization routines. Pros are that it is already written, and usually there are good documentation in libraries such as SciPy. Cons in this situation is, that most minimization routines are not able to handle multiple criteria at once. A work around is to combine the criteria into one single criteria by e.g. adding them quadratically and minimize that expression instead. The minimization routines are also not physical in the sense that they are not optimized for the problem. These two cons was incitement for writing a minimization optimized for our problem. Here is how it works.

1. Run MOOG once with a user defined initial parameters (default is solar) and calculate a_{EP} , a_{RW} , and ΔFe .
2. Change the atmospheric parameters (T_{eff} , $\log g$, $[\text{Fe}/\text{H}]$, ξ_{micro}) according to the size of the indicator. A parameter is only changed if it is not fixed.
 - a_{EP} : Indicator for T_{eff} . If this value is positive, then increase T_{eff} .
 - a_{RW} : Same as above but for ξ_{micro} .
 - ΔFe : Same as above but for $\log g$. Positive ΔFe means $\log g$ should be decreased.

² <http://scipy.org>

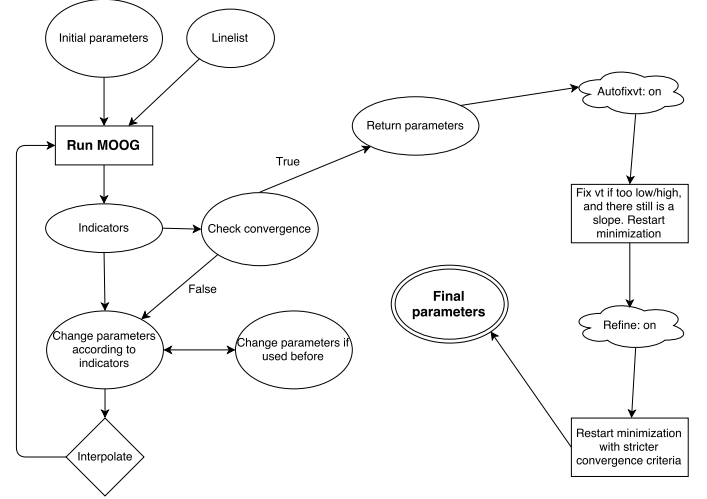


Fig. 2. A schematic overview over the minimization for MOOGme with the EW method.

3. For $[\text{Fe}/\text{H}]$ it is changed to the output $[\text{Fe}/\text{H}]$ in each iteration (if free).
4. If the new parameters have already been used in a previous, then change them slightly. This is done by drawing a random number from a Gaussian distribution with a mean at the previous value and a sigma equal to the absolute value of the indicator.
5. Calculate a new atmospheric model by interpolating a grid so we have the requested parameters and run MOOG once again.
6. For each iteration save the parameters used and the quadratic sum of the indicators. If we do not reach convergence, then return the best found parameters.

By using the indicators like this, we can relative fast reach convergence. There are some interdependencies among the indicators. E.g. by changing T_{eff} all indicators will be affected, however the effect is strongest for a_{EP} .

2.2.1. Options

It is possible to run the EW method with a set of different options which will be described here.

- *fixteff*: Fix T_{eff} . Same is available for $\log g$ (*fixlogg*), $[\text{Fe}/\text{H}]$ (*fixfeh*), and ξ_{micro} (*fixvt*).
- *outlier*: Remove outliers after the first run with the minimization routine and restarting the minimization from the previous best parameters. The options are to remove all outliers above 3σ once or iteratively, or remove one outlier above 3σ once or iteratively.
- *autofixvt*: If the minimization routine does not converge and ξ_{micro} is close to 0 or 10 with a significant a_{RW} , then fix ξ_{micro} .
- *refine*: After the minimization is done, run it again from the best found parameters but with more strict criteria. If this option is set, it will always be the last step (after removal of outliers and the use of *teffrange*).

If ξ_{micro} is fixed it is changed at each iteration according to an empirical relation. For dwarfs it follows the one presented in Tsantaki et al. (2013) and for giants it follows the one presented in Adibekyan et al. (2015). We use the line list presented in Sousa et al. (2008) for stars. However, this line list does not work well

for cool stars. This was fixed by Tsantaki et al. (2013) removing some lines from Sousa et al. (2008). For stars cooler than 5200 K we rederive the atmospheric parameters after removing lines so the line list resemble that of Tsantaki et al. (2013).

All restarts of the minimization routine is done with initial condition at the last found best parameters.

2.3. Abundance method

We made a mode to calculate abundances for different elements based on the measured EW. Here we require a line list with the EW of the elements and the corresponding atmospheric parameters for the star of interest. We provide a line list with XXX elements ready to use. The results are saved to a table.

2.4. Testing MOOGme

To test the EW method implemented in MOOGme we derive parameters from the 582 sample by Sousa et al. (2011). We use ARES2 to measure the EWs. ARES can give an estimate on the signal to noise ratio (SNR) by analyzing the continuum in given intervals. For solar type stars the following intervals are working well: 5764-5766 Å, 6047-6053 Å, and 6068-6076 Å. From the estimated SNR, ARES can give an estimate on the very important *rejt* parameters (see Sousa et al. 2015, for more information). After measuring the EWs with ARES, we use the MOOGme minimization described in Section 2.2 to determine the stellar atmospheric parameters. The results are presented in Figure 3 which shows T_{eff} , $\log g$, [Fe/H], and ξ_{micro} for MOOGme against those of Sousa et al. (2011).

The sample contains stars with T_{eff} too cold for the line list used. As described in Section 2.2 we should then apply the *tefrange* option to compensate by converting the normal line list by Sousa et al. (2008) to the line list presented in Tsantaki et al. (2013). However, this line list was not available when Sousa et al. (2011) derived parameters, hence we do not apply this option in order to make a better test for MOOGme.

The mean of the difference between parameters from Sousa et al. (2011) and those by MOOGme is presented in Table 1.

Table 1. The difference in derived parameters by Sousa et al. (2011) and MOOGme.

Parameter	Mean difference	Mean difference (same line list)
T_{eff}	16 ± 36 K	21 ± 11 K
$\log g$	-0.04 ± 0.07	-0.007 ± 0.009
[Fe/H]	0.03 ± 0.02	0.004 ± 0.009
ξ_{micro}	-0.04 ± 0.14 km/s	0.04 ± 0.02 km/s

We see small offsets that can be due to different versions of MOOG, different line lists, and different minimization routine. We therefore randomly selected 20 stars with different T_{eff} and used the line list directly from Sousa et al. (2011) to derive parameters. The results are presented in the last column of Table 1. We note that the $\log gf$ values from the original line lists by Sousa et al. (2011), which used the MOOG 2002 version, were not changed for the 2014 version of MOOG. This might lead to some errors as well. However, the offsets are very small and compatible with the errors on parameters normally obtained from high quality spectra.

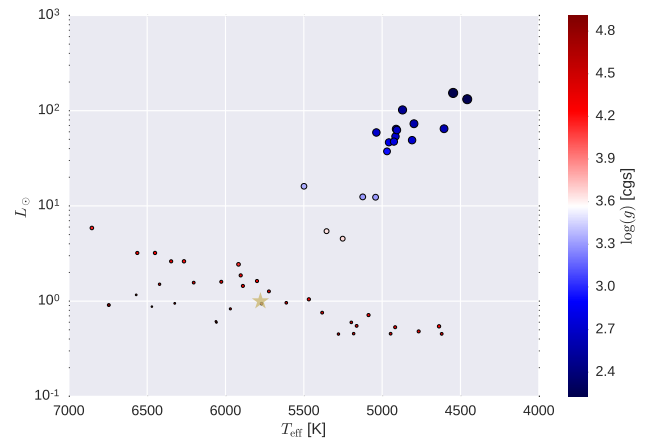


Fig. 4. Hertzsprung-Russell diagram of our sample with the Sun as a yellow star. The size of the points represents the $\log g$, with bigger points being smaller $\log g$ (giants), and vice versa. The colour code show the same as the size. Red points are the dwarfs, while blue points are the giants.

2.5. Web interface

We provide a web interface for MOOGme. In the web interface it is possible to use some of the line list provided with MOOGme to measure EWs of a spectrum (has to be provided by the user). This can be used for all the available MOOGme methods described above.

The web interface can be found at the following link [super-cool-address-with-MOOGme](#).

3. New spectroscopic parameters for 49 planet hosts

Here we present the sample of 50 stars. We were unable to derive parameters for HD77065. This is a spectroscopic binary according to Pourbaix et al. (2004).

The remaining 49 stars are presented in Table 2.

We present a Hertzsprung-Russell diagram (HRD) of our sample in Figure 4.

Figure 4 is made with a tool for post processing the results saved to a table by MOOGme. We also use *isochrones* (Morton 2015) to give an estimate of the age. The mass estimation is based on the relation by Torres et al. (2010). The age estimation is dependent on the mass of the star and the metallicity, which can be seen Figure 5.

4. Conclusion

Acknowledgements. This work was supported by Fundação para a Ciência e a Tecnologia (FCT) through the research grants UID/FIS/04434/2013 and PTDC/FIS-AST/1526/2014. N.C.S., and S.G.S. acknowledge the support from FCT through Investigador FCT contracts of reference IF/00169/2012, and IF/00028/2014, respectively, and POPH/FSE (EC) by FEDER funding through the program “Programa Operacional de Factores de Competitividade - COMPETE”. E.D.M. and B.J.A. acknowledge the support from FCT in form of the fellowship SFRH/BPD/76606/2011 and SFRH/BPD/87776/2012, respectively. This work also benefit from the collaboration of a cooperation project FCT/CAPES - 2014/2015 (FCT Proc 4.4.1.00 CAPES). AM received funding from the European Union Seventh Framework Programme (FP7/2007-2013) under grant agreement number 313014 (ETA-EARTH). This research has made use of the SIMBAD database operated at CDS, Strasbourg (France).

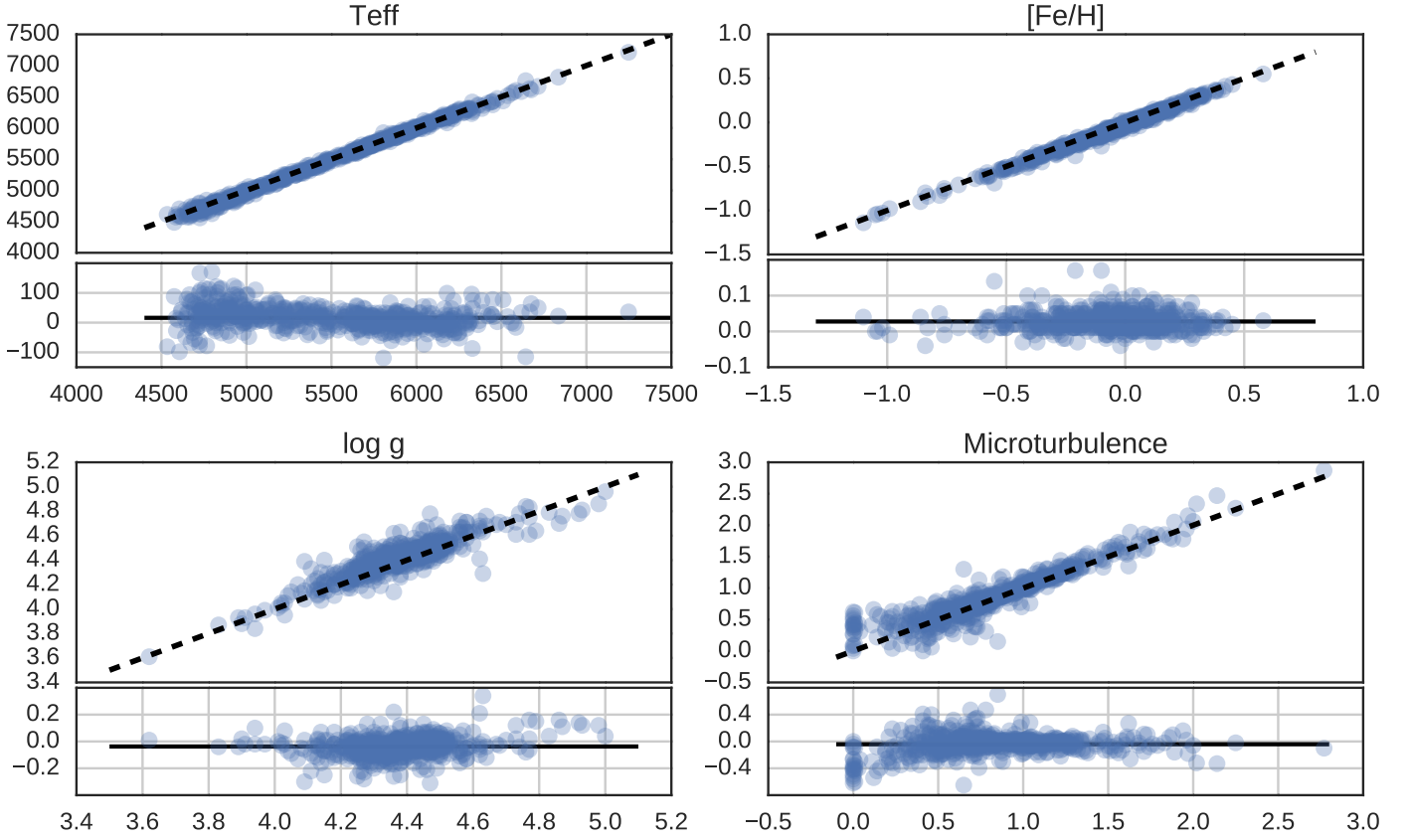


Fig. 3. Stellar atmospheric parameters derived by MOOGme compared to the sample by Sousa et al. (2011).

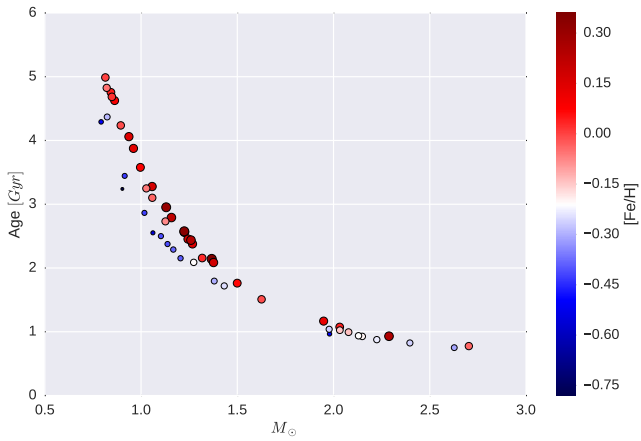


Fig. 5. Age versus mass for our sample, with colours representing the $[\text{Fe}/\text{H}]$.

References

- Adibekyan, V. Z., Benamati, L., Santos, N. C., et al. 2015, *MNRAS*, 450, 1900
 Kurucz, R. 1993, *ATLAS9 Stellar Atmosphere Programs and 2 km/s grid*. Kurucz CD-ROM No. 13. Cambridge, Mass.: Smithsonian Astrophysical Observatory, 1993., 13
 Morton, T. D. 2015, *isochrones: Stellar model grid package*, Astrophysics Source Code Library
 Morton, T. D., Bryson, S. T., Coughlin, J. L., et al. 2016, *ApJ*, 822, 86
 Pourbaix, D., Tokovinin, A. A., Batten, A. H., et al. 2004, *A&A*, 424, 727

- Santos, N. C., Sousa, S. G., Mortier, A., et al. 2013, *A&A*, 556, A150
 Sneden, C. A. 1973, PhD thesis, THE UNIVERSITY OF TEXAS AT AUSTIN.
 Sousa, S. G., Santos, N. C., Adibekyan, V., Delgado-Mena, E., & Israelian, G. 2015, *A&A*, 577, A67
 Sousa, S. G., Santos, N. C., Israelian, G., Mayor, M., & Udry, S. 2011, *A&A*, 533, A141
 Sousa, S. G., Santos, N. C., Mayor, M., et al. 2008, *A&A*, 487, 373
 Torres, G., Andersen, J., & Giménez, A. 2010, *A&A Rev.*, 18, 67
 Torres, G., Fischer, D. A., Sozzetti, A., et al. 2012, *ApJ*, 757, 161
 Tsantaki, M., Sousa, S. G., Adibekyan, V. Z., et al. 2013, *A&A*, 555, A150

Table 2. The derived parameters for the 49 stars in our sample.

Star	T_{eff} (K)	$\log g$ (dex)	[Fe/H] (dex)	ξ_{micro} (km/s)	ξ_{micro} fixed?	Program ID
WASP-76	6347 ± 52	4.29 ± 0.08	0.36 ± 0.04	1.73 ± 0.06	no	2014B/020, 094.C-0367
WASP-82	6563 ± 55	4.29 ± 0.10	0.18 ± 0.04	1.93 ± 0.08	no	2014B/020, 094.C-0367
WASP-88	6450 ± 61	4.24 ± 0.06	0.03 ± 0.04	1.79 ± 0.09	no	2014B/020, 095.C-0324
WASP-95	5799 ± 31	4.29 ± 0.05	0.22 ± 0.03	1.18 ± 0.04	no	2014B/020, 095.C-0324
WASP-97	5723 ± 52	4.37 ± 0.07	0.31 ± 0.04	1.03 ± 0.08	no	2014B/020, 094.C-0367
WASP-99	6324 ± 89	4.70 ± 0.11	0.27 ± 0.06	1.83 ± 0.12	no	2014B/020, 094.C-0367
HATS-1	5969 ± 46	4.61 ± 0.06	−0.04 ± 0.04	1.06 ± 0.08	no	092.C-0695
Qatar-2	4637 ± 316	4.23 ± 0.61	0.09 ± 0.17	0.63 ± 0.83	no	092.C-0695
WASP-44	5612 ± 80	4.47 ± 0.30	0.17 ± 0.06	1.32 ± 0.13	no	092.C-0695
HAT-P-46	6421 ± 121	4.53 ± 0.14	0.16 ± 0.09	1.67 ± 0.18	no	093.C-0219
WASP-52	5197 ± 83	4.47 ± 0.30	0.15 ± 0.05	1.16 ± 0.14	no	093.C-0219
WASP-72	6570 ± 85	4.71 ± 0.13	0.15 ± 0.06	2.30 ± 0.15	no	093.C-0219
WASP-75	6203 ± 46	4.42 ± 0.22	0.24 ± 0.03	1.45 ± 0.06	no	093.C-0219
HAT-P-42	5903 ± 66	4.29 ± 0.10	0.34 ± 0.05	1.19 ± 0.08	no	094.C-0367
HATS-5	5383 ± 91	4.40 ± 0.22	0.08 ± 0.06	0.91 ± 0.14	no	094.C-0367
HD 285507	4620 ± 126	4.42 ± 0.61	0.04 ± 0.06	0.74 ± 0.43	no	094.C-0367
HR 228	5042 ± 42	3.30 ± 0.09	0.07 ± 0.03	1.14 ± 0.04	no	094.C-0367
SAND364	4457 ± 104	2.26 ± 0.20	−0.04 ± 0.06	1.60 ± 0.11	no	094.C-0367
GJ 785	5087 ± 48	4.30 ± 0.10	−0.01 ± 0.03	0.69 ± 0.10	no	60.A-9036(A), 072.C-0488(E), 081.C-0842(D), 14AF14
HD 120084	4969 ± 40	2.94 ± 0.14	0.12 ± 0.03	1.41 ± 0.04	no	087.C-0012(B), 192.C-0852(A)
HD 192263	4946 ± 46	4.43 ± 0.14	−0.05 ± 0.02	0.66 ± 0.12	no	085.C-0062(A)
HIP 107773	4957 ± 49	2.83 ± 0.09	0.04 ± 0.04	1.49 ± 0.05	no	07bo03
HD 219134	4767 ± 70	4.32 ± 0.17	−0.00 ± 0.04	0.59 ± 0.24	no	14AF14, 53-202
HD 81688	4906 ± 29	2.69 ± 0.06	−0.21 ± 0.02	1.60 ± 0.03	no	14AF14, 53-202
HD 82886	5124 ± 22	3.30 ± 0.05	−0.25 ± 0.02	1.15 ± 0.03	no	11AQ78, 05AC23, 06AF22
mu Leo	4605 ± 94	2.61 ± 0.26	0.25 ± 0.06	1.64 ± 0.11	no	14AF14
HD 87883	4917 ± 68	4.34 ± 0.19	0.02 ± 0.03	0.46 ± 0.21	no	072.C-0488(E), 089.C-0732(A), 091.C-0034(A)
HIP 11915	5770 ± 14	4.47 ± 0.03	−0.06 ± 0.01	0.95 ± 0.02	no	14AF14
omi UMa	5499 ± 52	3.36 ± 0.07	−0.01 ± 0.05	1.98 ± 0.06	no	53-202
11 Com	4911 ± 38	2.68 ± 0.08	−0.20 ± 0.03	1.56 ± 0.04	no	53-202
HD 102272	5037 ± 80	2.72 ± 0.25	−0.52 ± 0.08	0.67 ± 0.12	no	53-202
HD 104985	4809 ± 48	2.73 ± 0.08	−0.26 ± 0.04	1.65 ± 0.05	no	53-202
HD 114762	6061 ± 83	4.70 ± 0.08	−0.78 ± 0.05	0.02 ± 0.26	no	53-202
omi CrB	4915 ± 33	2.74 ± 0.08	−0.14 ± 0.03	1.57 ± 0.04	no	53-202
HD 152581	5355 ± 82	3.65 ± 0.18	−0.39 ± 0.07	0.60 ± 0.15	no	095.C-0324, 53-202
HD 155358	5917 ± 51	4.12 ± 0.08	−0.55 ± 0.04	1.06 ± 0.08	no	40-203
42 Dra	4547 ± 55	2.23 ± 0.10	−0.31 ± 0.03	1.54 ± 0.05	no	49-202
HD 220842	6027 ± 30	4.35 ± 0.05	−0.08 ± 0.03	1.19 ± 0.04	no	44-210
14 And	4797 ± 44	2.58 ± 0.11	−0.23 ± 0.03	1.58 ± 0.04	no	49-202
HD 233604	4925 ± 44	2.79 ± 0.11	−0.15 ± 0.03	1.62 ± 0.05	no	53-202
HD 37124	5468 ± 32	4.28 ± 0.04	−0.43 ± 0.03	0.67 ± 0.07	no	53-202
HD 97658	5182 ± 43	4.50 ± 0.12	−0.29 ± 0.03	0.77 ± 0.11	no	53-202
Kepler-444	5163 ± 40	4.41 ± 0.11	−0.50 ± 0.03	0.78 ± 0.10	no	53-202
WASP-100	6853 ± 209	4.15 ± 0.26	−0.30 ± 0.12	1.87 ± 0.02	yes	2014B/020 094.C-0367
HAT-P-24	6470 ± 181	4.75 ± 0.26	−0.41 ± 0.10	1.40 ± 0.03	yes	092.C-0695
HAT-P-39	6745 ± 236	4.91 ± 0.46	−0.21 ± 0.12	1.53 ± 0.04	yes	094.C-0367
WASP-61	6265 ± 168	4.21 ± 0.21	−0.38 ± 0.11	1.44 ± 0.02	yes	094.C-0367
HD 70573	5889 ± 186	4.32 ± 0.27	−0.42 ± 0.13	1.14 ± 0.01	yes	53-202